Stabilizing the Exotic Carbonic Acid by Bisulfate Ion

Huili Lu [1], Shi-Wei Liu [2], Mengyang Li [4], Baocai Xu [3],*, Li Zhao [3], Tao Yang [4],* and Gao-Lei Hou [4],*

[1] Master Kong Beverage R&D Center, Shanghai 201103, China; luhuili@masterkong.com.cn
[2] China National Research Institute of Food & Fermentation Industries Co., Ltd., Beijing 100015, China; ff_nns@163.com
[3] School of Light Industry, Beijing Technology and Business University, Beijing 100048, China; zhaol@btbu.edu.cn
[4] MOE Key Laboratory for Non-Equilibrium Synthesis and Modulation of Condensed Matter, School of Physics, Xi'an Jiaotong University, Xi'an 710049, China; lmy0916@stu.xjtu.edu.cn
* Correspondence: xubaoc@btbu.edu.cn (B.X.); taoyang1@xjtu.edu.cn (T.Y.); chemglhou@gmail.com (G.-L.H.)

Abstract: Carbonic acid is an important species in a variety of fields and has long been regarded to be non-existing in isolated state, as it is thermodynamically favorable to decompose into water and carbon dioxide. In this work, we systematically studied a novel ionic complex $[H_2CO_3 \cdot HSO_4]^-$ using density functional theory calculations, molecular dynamics simulations, and topological analysis to investigate if the exotic H_2CO_3 molecule could be stabilized by bisulfate ion, which is a ubiquitous ion in various environments. We found that bisulfate ion could efficiently stabilize all the three conformers of H_2CO_3 and reduce the energy differences of isomers with H_2CO_3 in three different conformations compared to the isolated H_2CO_3 molecule. Calculated isomerization pathways and ab initio molecular dynamics simulations suggest that all the optimized isomers of the complex have good thermal stability and could exist at finite temperatures. We also explored the hydrogen bonding properties in this interesting complex and simulated their harmonic infrared spectra to aid future infrared spectroscopic experiments. This work could be potentially important to understand the fate of carbonic acid in certain complex environments, such as in environments where both sulfuric acid (or rather bisulfate ion) and carbonic acid (or rather carbon dioxide and water) exist.

Keywords: carbonic acid; bisulfate ion; density functional theory calculations; molecular dynamics simulations

1. Introduction

Carbonic acid, H_2CO_3, is a diprotic oxyacid and has long been considered as non-existing in isolated state [1]. Its importance in a range of fields, including astrophysics, astrobiology, astrochemistry, geography, and biochemistry, has been well-recognized [2–7]. It is of great significance in regulating blood pH, in adjusting ocean acidification, and in the dissolution of carbonate minerals [8]. In recent years, its potential as an interstellar molecule on the Martian surface, comets, and icy grain mantles has also attracted a lot of attention since both decomposition components of carbonic acid (i.e., carbon dioxide and water) have been discovered in those environments [4,5,9].

The non-existence of carbonic acid in isolated state was thought to be due to the fact that it is thermodynamically favorable to decompose into water and carbon dioxide, although theoretical calculations indicated that it might be kinetically trapped by a potential well [10,11]. The decomposition of carbonic acid could be efficiently promoted by a variety of species, such as water, ammonia, sulfuric acid, organics, and cloud particle surfaces. That could be one reason why isolated H_2CO_3 has escaped direct detection for a long time [11–17]. In 1987, Schwarz and co-workers reported the first observation of isolated H_2CO_3 via neutralization-reionization mass spectrometry of heated ammonium bicarbonate (NH_4HCO_3) vapor [1]. More than 20 years later, Endo and co-workers first spectroscopically detected both the *cis-trans* H_2CO_3 molecule in 2009 and the *cis-cis* H_2CO_3 molecule in 2011

using Fourier-transform microwave spectroscopy; the two H_2CO_3 isomers were produced via supersonic expansion and pulsed electric discharge of a carbon dioxide and water mixture [18,19]. In 2011, Bernard et al. also detected the two isomers of H_2CO_3 with the *cis-trans* isomer being less stable than the *cis-cis* one by about 4 kJ/mol and showed that H_2CO_3 is stable at temperatures above 200 K [20]. Later in 2014, Schreiner and co-workers reported a novel and general approach to prepare H_2CO_3 and its monomethyl ester (CH_3OCO_2H) through gas-phase pyrolysis of di-tert-butyl and tert-butyl methyl carbonate, respectively [21]. Furthermore, they verified that the previously thought polymorph of solid carbonic acid α-H_2CO_3 actually belongs to the carbonic acid monomethyl ester, and the β-polymorph is true H_2CO_3. Very recently, Ioppolo et al. provided evidence that β-H_2CO_3 should be ubiquitously present in space on the surface of CO_2- and H_2O-rich ices. They also observed unique spectral features of γ-H_2CO_3, deserving future search in the coldest regions of the interstellar medium [22]. Moreover, Wang et al. found that carbonic acid can even be formed from CO_2 on ice in the absence of high-energy irradiation and without protonation by strong acids, implying its potential role in the upper troposphere in cirrus clouds [23].

Hydrogen bonding is an effective way to stabilize otherwise unstable and uncommon structures [24–34]. For example, Hou et al. have performed a series of studies on bisulfate ion-containing complexes, showing that hydrogen bonding interactions can alter the protonation pattern in the complex, which violates the gas-phase proton affinity prediction [24,27,35–38]. This motivated us to wonder whether an appropriate partner such as bisulfate ion could also stabilize the exotic conformers of H_2CO_3 molecule. In fact, Thomas et al. has recently measured the infrared spectrum of the carbonic acid–fluoride complex anion in helium nanodroplets and found remarkable stability of $F^-(H_2CO_3)$ with carbonic acid in a *trans-trans* conformation [39]. Similar work on the whole series of carbonic acid–halide complexes, $X^-(H_2CO_3)$ (X = F, Cl, Br, and I), has been followed by Zhang et al. through joint photoelectron spectroscopy and ab initio calculations [40]. Here in this work, we theoretically studied the carbonic acid–bisulfate ion complex by using density functional theory (DFT) calculations and molecular dynamics simulations. The stability and bonding property of the complex have been explored.

2. Theoretical Methods

Geometry optimizations of all minima and transition states on the potential energy surface of the anionic molecular complex $[H_2CO_3 \cdot HSO_4]^-$ were performed by using DFT calculations. Specifically, M06-2X functional and aug-cc-pVTZ basis set were employed, as previous studies showed that this combination could provide reliable results for hydrogen bonded, bisulfate ion-containing complexes [24,27,35,36]. Harmonic frequency analysis was conducted at the same level of theory. All the quantum chemical calculations were performed with Gaussian09 program [41]. The natural bond orbital (NBO) analyses were carried out at M06-2X/aug-cc-pVTZ level using NBO 3.1 as implemented in Gaussian09. Ab initio molecular dynamics (AIMD) simulations using the Nosé-Hoover heat bath scheme with the average temperature of the system at 300, 400, 500, and 1000 K were performed for the most stable isomer, and an average temperature of 300 K for the second most stable isomer, with the Vienna ab initio simulation package (VASP) [42–44]. The PBE functional was used for the exchange-correlation functional [45]. A unit cell of 30 × 30 × 30 Å has been employed to avoid spurious interaction in space and the reciprocal space was represented by the Gamma point. The plane wave cut-off energy in the wave vector K space was 520 eV with the convergence criteria for the energy as 1×10^{-4} eV. Quantum theory of atoms in molecules (QTAIM) [46] analyses were also performed with Mutiwfn software [47] to gain insights into the H-bonding interactions in $[H_2CO_3 \cdot HSO_4]^-$.

3. Results and Discussion

Figure 1 presents the optimized low-lying isomers of $[H_2CO_3 \cdot HSO_4]^-$. To better understand the changes of each component in $[H_2CO_3 \cdot HSO_4]^-$ upon complexation, we

provide the optimized three conformers of carbonic acid, bisulfate ion, and sulfuric acid in Figure S1. It can be seen that the optimized structures of the three conformers are in good agreement with previous studies, and their relative stabilities are also consistent with previous calculations at a higher level of theory CCSD(T)/cc-pVQZ [10,11,18], verifying the reliability of the theoretical method utilized in the current work. For $[H_2CO_3 \cdot HSO_4]^-$, we have obtained six stable isomers, among which isomers **2a** and **2b** could be considered as enantiomers, and isomers **3a** and **3b** could also be considered as enantiomers. While isomers **1**, **3**, and **4** may be regarded as $HSO_4^- \cdot H_2CO_3$, isomer **2** is better recognized as $H_2SO_4 \cdot HCO_3^-$, which is only about 2 kJ/mol higher in energy than isomer **1**. Isomer **2** is unexpected solely from gas-phase proton affinity prediction and its stability can be attributed to the formation of two strong hydrogen bonds and highly delocalized extra electrons according to previous findings by Hou et al. [24,27,36–38]. Such electron delocalization can be partly reflected by the highest occupied molecular orbitals (HOMOs) as presented in Figure S2. Since we are mainly interested in understanding if bisulfate ion could stabilize carbonic acid molecule, in the following we will focus on isomers **1**, **3**, and **4**.
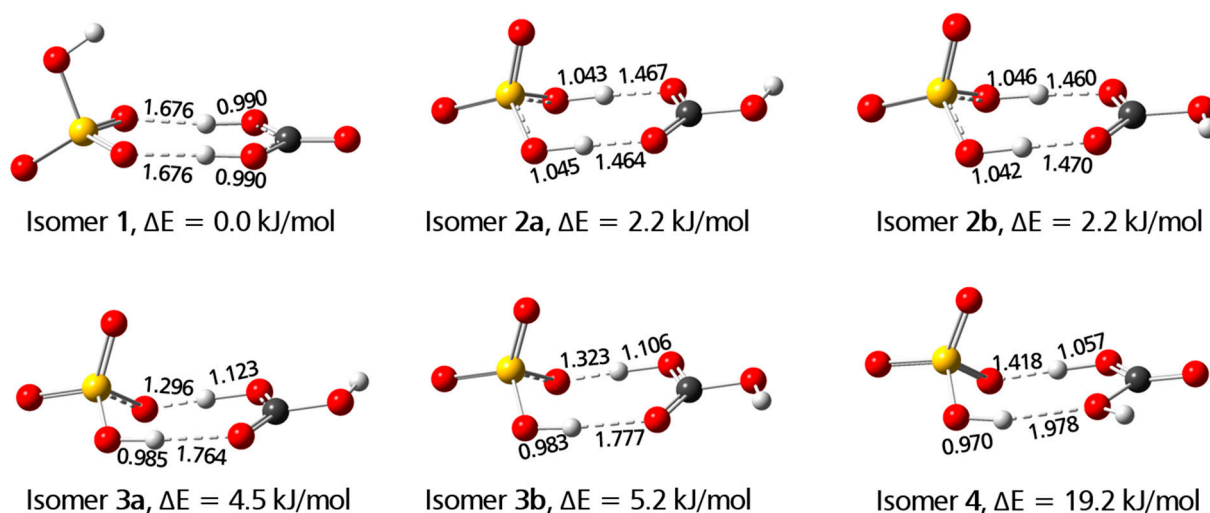

Figure 1. Optimized low-lying isomers of $[H_2CO_3 \cdot HSO_4]^-$ at M06-2X/aug-cc-pVTZ level of theory. Isomers **2a** and **2b** are energy degenerate, and isomers **3a** and **3b** are also energy degenerate.

It is interesting to note that in isomers **1**, **3a**, **3b**, and **4**, carbonic acid moiety is in the form of *trans-trans*, *cis-trans*, *cis-cis*, and *cis-trans*, respectively. For bare carbonic acid, *cis-cis* conformer is the most stable one, and *cis-trans* and *trans-trans* are higher in energy by 6.1 and 41.2 kJ/mol, respectively. Upon complexation with bisulfate ion, the isomer with carbonic acid moiety in *trans-trans* becomes to be the most stable one, which could be due to the formation of two equivalent hydrogen bonds. The energy differences of isomers with carbonic acid moiety in *cis-trans* and *cis-cis* relative to the most stable *trans-trans* one are much smaller compared in the bare case, suggesting the efficient stabilization of carbonic acid molecule by bisulfate ion. The smaller energy difference implies that these isomers may convert to each other upon gaining sufficient perturbation (for example, by thermionic heating or photoabsorption).

In Figure 2, we present the isomerization pathways between the different isomers of $[H_2CO_3 \cdot HSO_4]^-$ and the energy barriers needed to be overcome. The calculations show that the isomerization between isomers **2a** and **2b**, isomers **3a** and **3b** involves the rotation of −OH group in bicarbonate or carbonic acid, and the barriers are almost equal to be 45.4 and 46.4 kJ/mol, respectively. Such relatively high energy barriers may preclude the isomerization between the enantiomers of **2** and **3**, and they may all exist at finite temperatures. Isomerization between isomers **2a** and **3a**, isomers **2b** and **3b** has low barriers of only about 8 kJ/mol, indicating that the proton translocation between the two negatively charged oxygen atoms should not be difficult, as found in $HCOO^- \cdot H^+ \cdot HSO_4^-$ [36,48].

Visually, it seems isomerization between isomer **4** and isomer **3b** is more likely due to the fact that they have same hydrogen bond pattern between the two partners. However, due to the low energy barrier of proton translocation, our calculations show that isomerization happens between isomers **4** and **2b** via a transition state **ts42b** in which a proton translocates to bisulfate ion moiety simultaneously with the H transfer. This isomerization process has a large barrier of about 140 kJ/mol which is likely mainly resulted from the H transfer, making the isomerization between isomers **4** and **2b** not likely under ambient conditions. Conversion between isomers **1** and **4** is a stepwise process via an intermediate state **in14**. The first step is the H transfer from the −SOH moiety to the O of HSO_4^- that connects to the H_2CO_3 via a OH–O hydrogen bond; this step has a high energy barrier of ~125 kJ/mol. The second step is the swing of the H of one −OH of the H_2CO_3 with a comparably lower barrier of about 56 kJ/mol. This stepwise process has been confirmed by intrinsic reaction coordinate (IRC) scan (Figure S3 in the Supplementary Material). The large barrier of the first step renders the isomerization to be only possible at elevated temperatures or heating conditions.
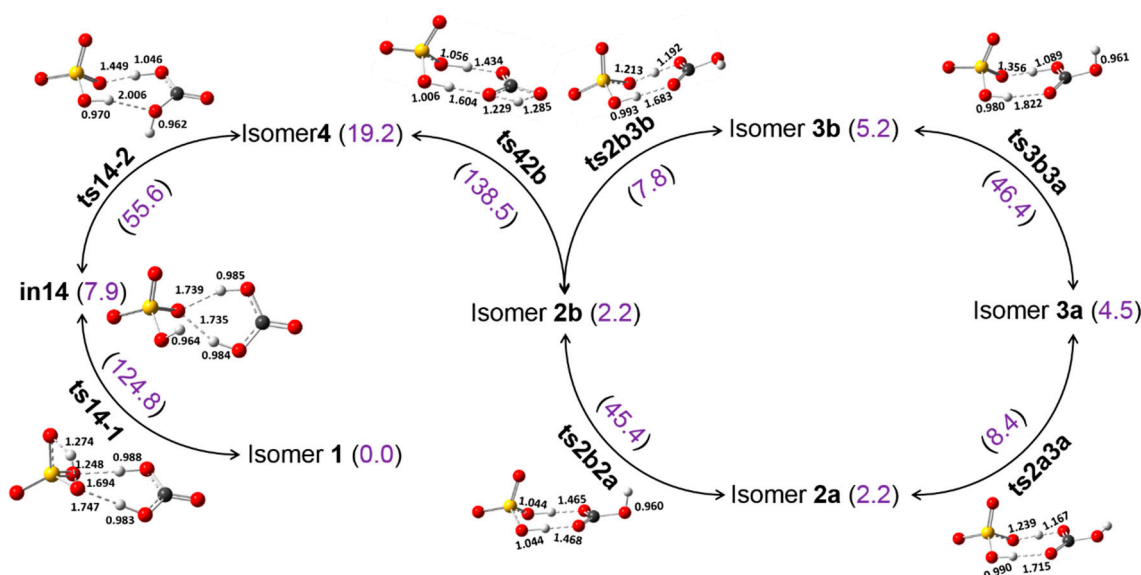
Figure 2. Calculated isomerization pathways between the different isomers of $[H_2CO_3 \cdot HSO_4]^-$. The optimized structures of transition states are provided, and the energy barriers are in kJ/mol in parenthesis.

To further evaluate the thermodynamical stability of the different isomers of $[H_2CO_3 \cdot HSO_4]^-$, we performed AIMD simulations for isomers **1** and **2a**, as presented in Figure 3. It can be seen that after 10,000 simulation steps (10 picoseconds), the structures of both isomers only show slight deformation compared to the ground state at 0 K, suggesting their high thermodynamic stability. Temperature and energy fluctuate over time in a steady-state, and the difference of the maximum and the minimum energies (ΔE) of isomer **1** and isomer **2a** are only about 0.5 eV, confirming their high-temperature stability [49,50]. We further simulated isomer **1** at higher temperatures of 400, 500, and 1000 K, all presenting its good stability (see animations in Figure S4).
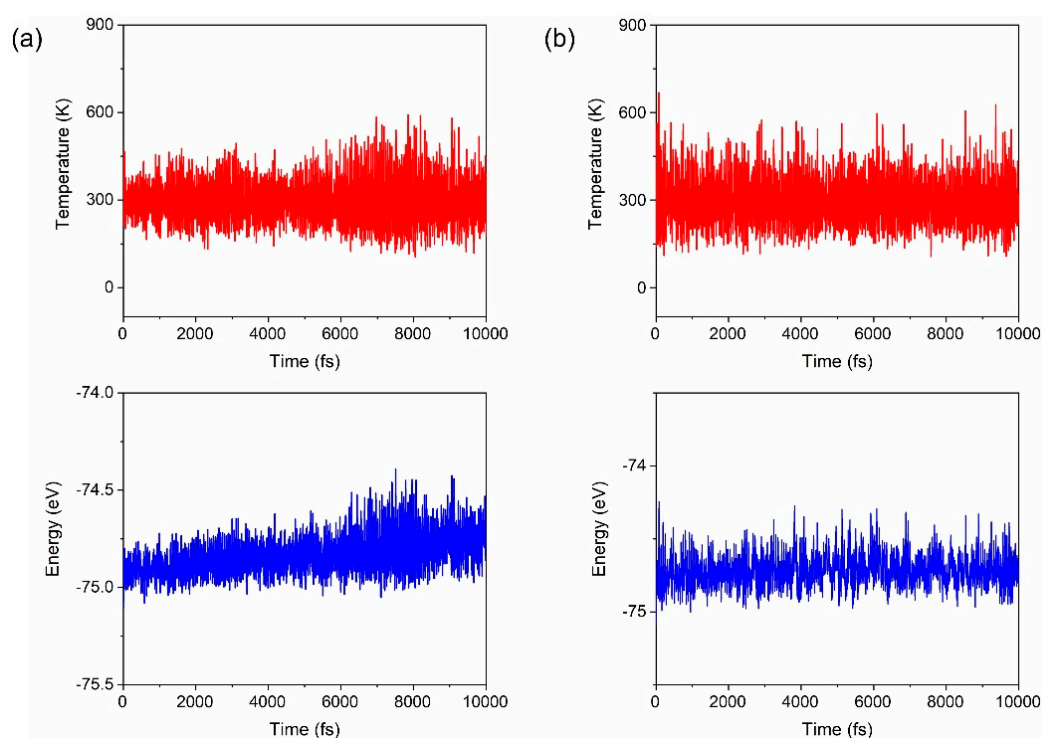
Figure 3. Total energy and temperature fluctuations with respect to time of the AIMD simulation for isomers **1** (**a**) and **2a** (**b**) both at 300 K.

As stated above, the high stability of those isomers comes from hydrogen bond formation and extra electron delocalization. The electron delocalization could partly be reflected by the HOMOs as shown in Figure S2 and partly by the charge distributions as summarized in Table S1. QTAIM is a useful approach to evaluate the nature of hydrogen bond and its strength in addition to the geometrical analysis [37,46]. According to Bader's theory, the critical points (3,−3) are the nuclear positions where the charge density is local maximum in all directions, and the BCPs (3,−1) correspond to the second-order saddle points, for which two eigenvalues of the charge density Hessian matrix are negative and one is positive. The BCPs and the nuclei are connected by the maximum charge density paths. Figure S5 presents the molecular graphs showing all the BCPs. The electron density (ρ) and its Laplacian ($\nabla^2 \rho$) at BCP are closely related to bonding strength and bonding type, respectively; the potential energy density (V(r)), gradient kinetic energy density (G(r)), and electronic energy density (K(r)) are highly correlated with the hydrogen bond energies. These values are summarized in Table 1.

Table 1. Electron density (ρ), Laplacian ($\nabla^2 \rho$), potential energy density (V(r)), gradient kinetic energy density (G(r)), and electronic energy density (K(r)) at BCPs of the hydrogen bonds in the different isomeric structures of $[H_2CO_3 \cdot HSO_4]^-$. All units are in a.u, except that E_{HB} is in kcal/mol.

| $[H_2CO_3 \cdot HSO_4]^-$	ρ (10^{-2}) [a]		$\nabla^2 \rho$ (10^{-2})		V(r) (10^{-2})		G(r) (10^{-2})		K(r) (10^{-2})		E_{HB}	
	I [b]	II	I	II	I	II	I	II	I	II	I	II
Isomer **1**	4.696	4.695	10.923	10.923	−4.960	−4.959	3.845	3.845	1.115	1.114	−16.67	−16.67
Isomer **2a**	8.397	8.454	7.844	7.692	−10.000	−10.087	5.980	6.005	4.019	4.082	−28.97	−29.16
Isomer **2b**	8.448	8.403	7.699	7.837	−10.080	−10.009	6.002	5.984	4.077	4.025	−29.14	−28.99
Isomer **3a**	12.889	3.760	−6.519	10.678	−17.922	−3.696	8.146	3.183	9.776	0.513	−43.90	−13.56
Isomer **3b**	11.976	3.629	−1.754	10.665	−16.088	−3.535	7.825	3.101	8.263	0.435	−40.87	−13.13
Isomer **4**	9.311	2.160	6.644	8.408	−11.505	−1.786	6.583	1.944	4.922	−0.158	−32.01	−8.24

[a] Positive values of ρ indicate closed-shell interactions between two hydrogen bonded atoms according to Koch and Popelier [51]. [b] See Figure S5 for the notation of hydrogen bonds I and II in each isomer.

From Table 1, it can be seen that the electron density distribution (ρ) and its Laplacian ($\nabla^2\rho$) at BCPs of the two hydrogen bonds of isomers **1** and **2** are almost identical, while those of isomers **3** and **4** differ a lot, consistent with the structural analyses. Such difference can also be seen from the values of electronic energy density K(r), whose magnitude is related to the hydrogen bond strength. In 2019, Emamian et al. investigated a series of hydrogen bonded complexes and fitted an equation $E_{HB} = -332.34 \times \rho_{BCP} - 1.0661$ to estimate the hydrogen bond energy (E_{HB}) for hydrogen bonded ionic complexes. This equation gives a mean absolute percentage error (MAPE, in kcal/mol) of 10.0%, and ρ_{BCP} is the electron density at the BCP of hydrogen bonds in a.u., and E_{HB} is in kcal/mol [52]. The hydrogen bond energies estimated in this way are summarized in Table 1, and it is shown clearly that the calculated hydrogen bond strengths are consistent with the optimized geometric structures (i.e., the shorter O–HO distance, the higher hydrogen bond energy).

Temperature-controlled infrared spectroscopy is a useful experimental approach to probe the proton translocation dynamics as demonstrated by Johnson and co-workers [53,54] and very recently also by von Helden and co-workers [39,48]. To guide future infrared spectroscopic experiments, we simulated the harmonic vibrational spectra of the six isomers of $[H_2CO_3 \cdot HSO_4]^-$, as presented in Figure 4.
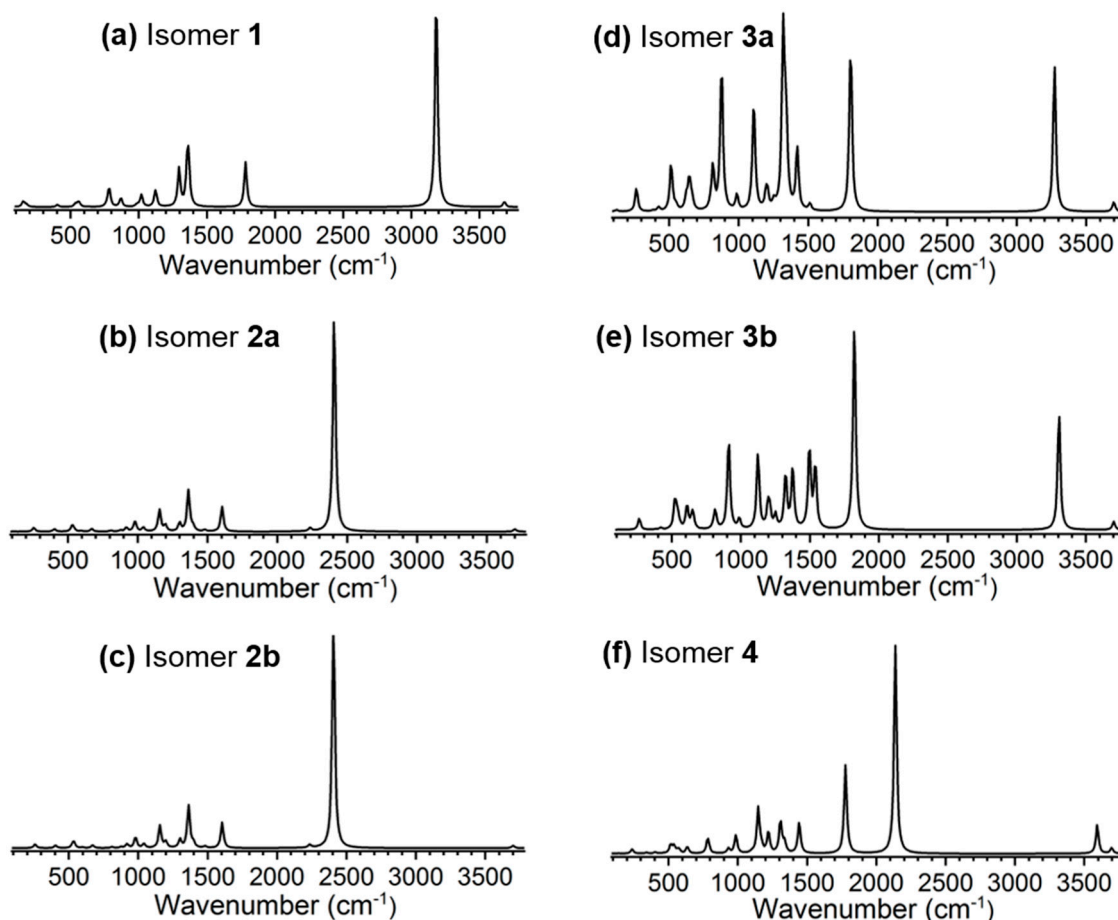
Figure 4. Simulated harmonic infrared spectra of the six isomers (**a–f**) of $[H_2CO_3 \cdot HSO_4]^-$ at M06-2X/aug-cc-pVTZ level of theory. The calculated vibrational frequencies have been broadened using Gaussian line shape of 12 cm^{-1} full width half maximum, and a scaling factor of 0.956 [55] has been applied.

In isomer 1, there is a very weak vibrational mode at ~3680 cm^{-1} corresponding to the O–H stretching of the HSO$_4^-$ moiety, and the strong vibration at ~3180 cm^{-1} is the symmetric double O–H stretching of the H$_2$CO$_3$ moiety. The spectra of isomers **2a** and **2b**

are almost identical, as they are enantiomers; the vibrations at ~2230 and 2410 cm^{-1} are the asymmetric and symmetric stretching of the two shared H$^+$ between SO$_4^{2-}$ and HCO$_3^-$ moieties. Similarly, the spectra of isomers **3a** and **3b** are almost identical; the weak mode at ~3700 cm^{-1} is the free O–H stretching of the H$_2$CO$_3$ moiety, and the two strong modes at ~1810 and 3270 cm^{-1} are the shared H$^+$ translocation and hydrogen bonded O–H stretching of the HSO$_4^-$ moiety. In the simulated spectrum of isomer **4**, the vibrations at ~2130, 3590, and 3700 cm^{-1} are the shared H$^+$ translocation, hydrogen bonded O–H stretching of the HSO$_4^-$ moiety, and the free O–H stretching of the H$_2$CO$_3$ moiety. Those vibrational vectors are included in Figure S6 in the Supplementary Materials. It should be mentioned that more accurate description of the vibrations in those structures requires more advanced theoretical treatments including both anharmonic effects and nuclear quantum effects, and is beyond the scope of current study [48].

4. Conclusions

In summary, we theoretically explored the potential energy surface of the anionic [H$_2$CO$_3$·HSO$_4$]$^-$ complex to investigate if bisulfate ion is capable to stabilize the exotic conformers of carbonic acid. Our results showed that compared to the bare H$_2$CO$_3$ molecule, the energy differences between the different isomers of [H$_2$CO$_3$·HSO$_4$]$^-$ complex with H$_2$CO$_3$ moiety in the conformation of *trans-trans*, *cis-trans*, and *cis-cis* become smaller, suggesting that bisulfate ion can efficiently stabilize the three conformers of H$_2$CO$_3$. Notably, for bare H$_2$CO$_3$, the *cis-cis* conformer is the most stable, while in [H$_2$CO$_3$·HSO$_4$]$^-$ the isomer with H$_2$CO$_3$ in *trans-trans* becomes the most stable due to the formation of two strong hydrogen bonds. Combining quantum theory of atoms in molecules topological analysis and a fitted empirical equation, we estimated the strengths of the hydrogen bonds. The calculated isomerization pathways between the different isomers of [H$_2$CO$_3$·HSO$_4$]$^-$ and also ab initio molecular dynamics simulations of the first two low-lying isomers revealed that these isomers could coexist at finite temperatures. We further simulated their harmonic infrared spectra to facilitate future infrared spectroscopic experiments to fully understand the proton translocation dynamics in this interesting complex.

Supplementary Materials: The following are available online. Figure S1: Three conformers of isolated carbonic acid molecule, bisulfate ion, and *cis-cis* sulfuric acid molecule; Figure S2: Molecular orbitals of the optimized isomers of [H$_2$CO$_3$·HSO$_4$]$^-$; Figure S3: Intrinsic reaction coordinate (IRC) scan for the stepwise conversion of isomer **1** to isomer **4** via an intermediate state **in14**; Figure S4: Animations showing the AIMD simulations for isomers **1** and **2a**; Figure S5: Molecular graphs of [H$_2$CO$_3$·HSO$_4$]$^-$; Figure S6: Vibrational vectors for the selected vibrational modes of the isomers of [H$_2$CO$_3$·HSO$_4$]$^-$; Figure S7: Vibrational vectors for the imaginary vibrational modes of the transition states of [H$_2$CO$_3$·HSO$_4$]$^-$; Table S1: Charge distributions from natural population analysis for the different isomers of [H$_2$CO$_3$·HSO$_4$]$^-$; Table S2: Cartesian coordinates.

Institutional Review Board Statement: Not applicable.

Informed Consent Statement: Not applicable.

Data Availability Statement: Not available.

Conflicts of Interest: The authors declare no conflict of interest.

Sample Availability: Samples of the compounds are not available from the authors.

References

1. Terlouw, J.K.; Lebrilla, C.B.; Schwarz, H. Thermolysis of NH_4HCO_3—A aimple route to the formation of free carbonic acid (H_2CO_3) in the gas phase. *Angew. Chem. Int. Ed.* **1987**, *26*, 354–355. [CrossRef]
2. Andersson, A.J.; Mackenzie, F.T.; Lerman, A. Coastal ocean CO_2-carbonic acid-carbonate sediment system of the Anthropocene. *Glob. Biogeochem. Cycles* **2006**, *20*, GB1S92. [CrossRef]
3. Stolte, N.; Pan, D. Large presence of carbonic acid in CO_2-rich aqueous fluids under earth's mantle conditions. *J. Phys. Chem. Lett.* **2019**, *10*, 5135–5141. [CrossRef] [PubMed]
4. Strazzulla, G.; Brucato, J.R.; Cimino, G.; Palumbo, M.E. Carbonic acid on Mars? *Planet. Space Sci.* **1996**, *44*, 1447–1450. [CrossRef]
5. Hage, W.; Liedl Klaus, R.; Hallbrucker, A.; Mayer, E. Carbonic acid in the gas phase and its astrophysical relevance. *Science* **1998**, *279*, 1332–1335. [CrossRef]
6. Delitsky, M.L.; Lane, A.L. Ice chemistry on the Galilean satellites. *J. Geophys. Res. Planets* **1998**, *103*, 31391–31403. [CrossRef]
7. Aminov, D.; Pines, D.; Kiefer, P.M.; Daschakraborty, S.; Hynes, J.T.; Pines, E. Intact carbonic acid is a viable protonating agent for biological bases. *Proc. Natl. Acad. Sci. USA* **2019**, *116*, 20837. [CrossRef]
8. Al-Hosney, H.A.; Grassian, V.H. Carbonic Acid: An important intermediate in the surface chemistry of calcium carbonate. *J. Am. Chem. Soc.* **2004**, *126*, 8068–8069. [CrossRef]
9. Moore, M.H.; Hudson, R.L.; Gerakines, P.A. Mid- and far-infrared spectroscopic studies of the influence of temperature, ultraviolet photolysis and ion irradiation on cosmic-type ices. *Spectrochim. Acta A Mol. Biomol. Spectrosc.* **2001**, *57*, 843–858. [CrossRef]
10. Jönsson, B.; Karlström, G.; Wennerström, H.; Roos, B. Ab initio molecular orbital calculations on the water-carbon dioxide system: Carbonic acid. *Chem. Phys. Lett.* **1976**, *41*, 317–320. [CrossRef]
11. Kumar, P.P.; Kalinichev, A.G.; Kirkpatrick, R.J. Dissociation of carbonic acid: Gas phase energetics and mechanism from ab initio metadynamics simulations. *J. Chem. Phys.* **2007**, *126*, 204315. [CrossRef] [PubMed]
12. Kumar, M.; Busch, D.H.; Subramaniam, B.; Thompson, W.H. Organic acids tunably catalyze carbonic acid decomposition. *J. Phys. Chem. A* **2014**, *118*, 5020–5028. [CrossRef] [PubMed]
13. Bandyopadhyay, B.; Biswas, P.; Kumar, P. Ammonia as an efficient catalyst for decomposition of carbonic acid: A quantum chemical investigation. *Phys. Chem. Phys. Chem.* **2016**, *18*, 15995–16004. [CrossRef] [PubMed]
14. Mallick, S.; Sarkar, S.; Bandyopadhyay, B.; Kumar, P. Effect of ammonia-water complex on decomposition of carbonic acid in troposphere: A quantum chemical investigation. *Comput. Theor. Chem.* **2018**, *1132*, 50–58. [CrossRef]
15. Ghoshal, S.; Hazra, M.K. $H_2CO_3 \rightarrow CO_2 + H_2O$ decomposition in the presence of H_2O, HCOOH, CH_3COOH, H_2SO_4 and HO_2 radical: Instability of the gas-phase H_2CO_3 molecule in the troposphere and lower stratosphere. *RSC Adv.* **2015**, *5*, 17623–17635. [CrossRef]
16. de Marothy, S.A. Autocatalytic decomposition of carbonic acid. *Int. J. Quantum Chem.* **2013**, *113*, 2306–2311. [CrossRef]
17. Ghoshal, S.; Hazra, M.K. New mechanism for autocatalytic decomposition of H_2CO_3 in the vapor phase. *J. Phys. Chem. A* **2014**, *118*, 2385–2392. [CrossRef]
18. Mori, T.; Suma, K.; Sumiyoshi, Y.; Endo, Y. Spectroscopic detection of isolated carbonic acid. *J. Chem. Phys.* **2009**, *130*, 204308. [CrossRef]
19. Mori, T.; Suma, K.; Sumiyoshi, Y.; Endo, Y. Spectroscopic detection of the most stable carbonic acid, *cis-cis* H_2CO_3. *J. Chem. Phys.* **2011**, *134*, 044319. [CrossRef] [PubMed]
20. Bernard, J.; Seidl, M.; Kohl, I.; Liedl, K.R.; Mayer, E.; Gálvez, Ó.; Grothe, H.; Loerting, T. Spectroscopic observation of matrix-isolated carbonic acid trapped from the gas phase. *Angew. Chem. Int. Ed.* **2011**, *50*, 1939–1943. [CrossRef]
21. Reisenauer, H.P.; Wagner, J.P.; Schreiner, P.R. Gas-phase preparation of carbonic acid and its monomethyl ester. *Angew. Chem. Int. Ed.* **2014**, *53*, 11766–11771. [CrossRef] [PubMed]
22. Ioppolo, S.; Kaňuchová, Z.; James, R.L.; Dawes, A.; Ryabov, A.; Dezalay, J.; Jones, N.C.; Hoffmann, S.V.; Mason, N.J.; Strazzulla, G.; et al. Vacuum ultraviolet photoabsorption spectroscopy of space-related ices: Formation and destruction of solid carbonic acid upon 1 keV electron irradiation. *Astron. Astrophys.* **2021**, *646*, A172. [CrossRef]
23. Wang, X.; Bgrgi, T. Observation of carbonic acid formation from interaction between carbon dioxide and ice by using in situ modulation excitation IR spectroscopy. *Angew. Chem. Int. Ed.* **2021**, *60*, 7860–7865. [CrossRef] [PubMed]
24. Hou, G.-L.; Wang, X.-B. Molecular specificity and proton transfer mechanisms in aerosol prenucleation clusters relevant to new particle formation. *Acc. Chem. Res.* **2020**, *53*, 2816–2827. [CrossRef] [PubMed]
25. Cao, W.; Zhang, H.; Yuan, Q.; Zhou, X.; Kass, S.R.; Wang, X.-B. Observation of conformational simplification upon N-methylation on amino acid iodide clusters. *J. Phys. Chem. Lett.* **2021**, *12*, 2780–2787. [CrossRef]
26. Wang, L.; Yuan, Q.; Cao, W.; Han, J.; Zhou, X.; Liu, S.; Wang, X.-B. Probing orientation-specific charge–dipole interactions between hexafluoroisopropanol and halides: A joint photoelectron spectroscopy and theoretical study. *J. Phys. Chem. A* **2020**, *124*, 2036–2045. [CrossRef]
27. Hou, G.-L.; Lin, W.; Wang, X.-B. Direct observation of hierarchic molecular interactions critical to biogenic aerosol formation. *Commun. Chem.* **2018**, *1*, 37. [CrossRef]

28. Wen, H.; Hou, G.-L.; Kathmann, S.M.; Valiev, M.; Wang, X.-B. Communication: Solute anisotropy effects in hydrated anion and neutral clusters. *J. Chem. Phys.* **2013**, *138*, 031101. [CrossRef]

29. Hou, G.-L.; Zhang, J.; Valiev, M.; Wang, X.-B. Structures and energetics of hydrated deprotonated cis-pinonic acid anion clusters and their atmospheric relevance. *Phys. Chem. Phys. Chem.* **2017**, *19*, 10676–10684. [CrossRef]

30. Hou, G.-L.; Liu, C.-W.; Li, R.-Z.; Xu, H.-G.; Gao, Y.Q.; Zheng, W.-J. Emergence of solvent-separated Na⁺–Cl⁻ ion pair in salt water: Photoelectron spectroscopy and theoretical calculations. *J. Phys. Chem. Lett.* **2017**, *8*, 13–20. [CrossRef]

31. Wen, H.; Hou, G.-L.; Liu, Y.-R.; Wang, X.-B.; Huang, W. Examining the structural evolution of bicarbonate–water clusters: Insights from photoelectron spectroscopy, basin-hopping structural search, and comparison with available IR spectral studies. *Phys. Chem. Phys. Chem.* **2016**, *18*, 17470–17482. [CrossRef]

32. Hou, G.-L.; Valiev, M.; Wang, X.-B. Deprotonated dicarboxylic acid homodimers: Hydrogen bonds and atmospheric implications. *J. Phys. Chem. A* **2016**, *120*, 2342–2349. [CrossRef]

33. Ferguson, S.J. Proton transfer: It's a stringent process. *Curr. Biol.* **2000**, *10*, R627–R630. [CrossRef]

34. Blake, R.S.; Monks, P.S.; Ellis, A.M. Proton-transfer reaction mass spectrometry. *Chem. Rev.* **2009**, *109*, 861–896. [CrossRef] [PubMed]

35. Hou, G.-L.; Lin, W.; Deng, S.H.M.; Zhang, J.; Zheng, W.-J.; Paesani, F.; Wang, X.-B. Negative ion photoelectron spectroscopy reveals thermodynamic advantage of organic acids in facilitating formation of bisulfate ion clusters: Atmospheric implications. *J. Phys. Chem. Lett.* **2013**, *4*, 779–785. [CrossRef]

36. Hou, G.-L.; Wang, X.-B.; Valiev, M. Formation of (HCOO⁻)(H₂SO₄) anion clusters: Violation of gas-phase acidity predictions. *J. Am. Chem. Soc.* **2017**, *139*, 11321–11324. [CrossRef]

37. Hou, G.-L.; Valiev, M.; Wang, X.-B. Sulfuric acid and aromatic carboxylate clusters H₂SO₄·ArCOO⁻: Structures, properties, and their relevance to the initial aerosol nucleation. *Int. J. Mass Spectrom.* **2019**, *439*, 27–33. [CrossRef]

38. Hou, G.-L.; Wang, X.-B. Spectroscopic signature of proton location in proton bound HSO₄⁻·H⁺·X⁻ (X = F, Cl, Br, and I) clusters. *J. Phys. Chem. Lett.* **2019**, *10*, 6714–6719. [CrossRef]

39. Thomas, D.A.; Mucha, E.; Lettow, M.; Meijer, G.; Rossi, M.; von Helden, G. Characterization of a trans–trans carbonic acid–fluoride complex by infrared action spectroscopy in helium nanodroplets. *J. Am. Chem. Soc.* **2019**, *141*, 5815–5823. [CrossRef] [PubMed]

40. Zhang, H.; Cao, W.; Yuan, Q.; Wang, L.; Zhou, X.; Liu, S.; Wang, X.-B. Spectroscopic evidence for intact carbonic acid stabilized by halide anions in the gas phase. *Phys. Chem. Phys. Chem.* **2020**, *22*, 19459–19467. [CrossRef]

41. Frisch, M.J.; Trucks, G.W.; Schlegel, H.B.; Scuseria, G.E.; Robb, M.A.; Cheeseman, J.R.; Scalmani, G.; Barone, V.; Petersson, G.A.; Nakatsuji, H.; et al. *Gaussian 09 (Revision E.01)*; Gaussian Inc.: Wallingford, CT, USA, 2013.

42. Kresse, G.; Furthmüller, J. Efficiency of ab-initio total energy calculations for metals and semiconductors using a plane-wave basis set. *Comput. Mater. Sci.* **1996**, *6*, 15–50. [CrossRef]

43. Kresse, G.; Furthmüller, J. Efficient iterative schemes for ab initio total-energy calculations using a plane-wave basis set. *Phys. Rev. B* **1996**, *54*, 11169–11186. [CrossRef] [PubMed]

44. Kresse, G.; Joubert, D. From ultrasoft pseudopotentials to the projector augmented-wave method. *Phys. Rev. B* **1999**, *59*, 1758–1775. [CrossRef]

45. Perdew, J.P.; Burke, K.; Ernzerhof, M. Generalized gradient approximation made simple. *Phys. Rev. Lett.* **1996**, *77*, 3865–3868. [CrossRef] [PubMed]

46. Bader, R.F.W. A quantum theory of molecular structure and its applications. *Chem. Rev.* **1991**, *91*, 893–928. [CrossRef]

47. Lu, T.; Chen, F. Multiwfn: A multifunctional wavefunction analyzer. *J. Comput. Chem.* **2012**, *33*, 580–592. [CrossRef]

48. Thomas, D.A.; Taccone, M.; Ober, K.; Mucha, E.; Meijer, G.; von Helden, G. Helium nanodroplet infrared action spectroscopy of the proton-bound dimer of hydrogen sulfate and formate: Examining nuclear quantum effects. *J. Phys. Chem. A* **2021**, *125*, 9279–9287. [CrossRef] [PubMed]

49. Zhao, H.; Zhou, J.; Jena, P. Stability of B₁₂(CN)₁₂²⁻: Implications for lithium and magnesium ion batteries. *Angew. Chem. Int. Ed.* **2016**, *55*, 3704–3708. [CrossRef]

50. Xu, J.; Li, M.; Xu, S.; Pei, G.; Zhao, X.; Kong, C.; Yang, Z.; Yang, T.; Hou, G.-L. Stable noble gas compounds based on superelectrophilic anions [B₁₂(BO)₁₁]⁻ and [B₁₂(OBO)₁₁]⁻. *ChemPhysChem* **2021**, *22*, 2240–2246. [CrossRef]

51. Koch, U.; Popelier, P.L.A. Characterization of C–H–O hydrogen bonds on the basis of the charge density. *J. Phys. Chem.* **1995**, *99*, 9747–9754. [CrossRef]

52. Emamian, S.; Lu, T.; Kruse, H.; Emamian, H. Exploring nature and predicting strength of hydrogen bonds: A correlation analysis between atoms-in-molecules descriptors, binding energies, and energy components of symmetry-adapted perturbation theory. *J. Comput. Chem.* **2019**, *40*, 2868–2881. [CrossRef] [PubMed]

53. Yang, N.; Duong, C.H.; Kelleher, P.J.; McCoy, A.B.; Johnson, M.A. Deconstructing water's diffuse OH stretching vibrational spectrum with cold clusters. *Science* **2019**, *364*, 275–278. [CrossRef] [PubMed]

54. Zeng, H.J.; Johnson, M.A. Demystifying the diffuse vibrational spectrum of aqueous protons through cold cluster spectroscopy. *Annu. Rev. Phys. Chem.* **2021**, *72*, 667–691. [CrossRef] [PubMed]

55. Available online: https://cccbdb.nist.gov/vibscalejust.asp (accessed on 30 November 2021).